

Continuously tunable solution-processed organic semiconductor DFB lasers pumped by laser diode

Sönke Klinkhammer,^{1,2,3} Xin Liu,^{1,2,3} Klaus Huska,¹ Yuxin Shen,^{1,5} Sylvia Vanderheiden,⁴ Sebastian Valouch,^{1,2} Christoph Vannahme,^{3,1,6} Stefan Bräse,⁴ Timo Mappes,³ and Uli Lemmer^{1,2,*}

¹Light Technology Institute (LTI), Karlsruhe Institute of Technology (KIT), 76128 Karlsruhe, Germany
²DFG-Center for Functional Nanostructures (CFN), Karlsruhe Institute of Technology (KIT), 76131 Karlsruhe, Germany

³Institute of Microstructure Technology (IMT), Karlsruhe Institute of Technology (KIT), 76128 Karlsruhe, Germany

⁴Institute for Organic Chemistry (IOC), Karlsruhe Institute of Technology (KIT), 76128 Karlsruhe, Germany

⁵currently with Novald AG, Dresden, Germany

⁶currently with DTU Nanotech, Lyngby, Denmark

*uli.lemmer@kit.edu

Abstract: The fabrication and characterization of continuously tunable, solution-processed distributed feedback (DFB) lasers in the visible regime is reported. Continuous thin film thickness gradients were achieved by means of horizontal dipping of several conjugated polymer and blended small molecule solutions on cm-scale surface gratings of different periods. We report optically pumped continuously tunable laser emission of 13 nm in the blue, 16 nm in the green and 19 nm in the red spectral region on a single chip respectively. Tuning behavior can be described with the Bragg-equation and the measured thickness profile. The laser threshold is low enough that inexpensive laser diodes can be used as pump sources.

©2012 Optical Society of America

OCIS codes: (140.3490) Lasers, distributed-feedback; (140.7300) Visible lasers; (250.2080) Polymer active devices.

References and links

1. N. Tessler, G. J. Denton, and R. H. Friend, "Lasing from conjugated-polymer microcavities," *Nature* **382**(6593), 695–697 (1996).
2. I. D. W. Samuel and G. A. Turnbull, "Organic semiconductor lasers," *Chem. Rev.* **107**(4), 1272–1295 (2007).
3. T. Riedl, T. Rabe, H. H. Johannes, W. Kowalsky, J. Wang, T. Weimann, P. Hinze, B. S. Nehls, T. Farrell, and U. Scherf, "Tunable organic thin-film laser pumped by an inorganic violet diode laser," *Appl. Phys. Lett.* **88**(24), 241116 (2006).
4. A. E. Vasdekis, G. Tsiminis, J.-C. Ribierre, L. O' Faolain, T. F. Krauss, G. A. Turnbull, and I. D. W. Samuel, "Diode pumped distributed Bragg reflector lasers based on a dye-to-polymer energy transfer blend," *Opt. Express* **14**(20), 9211–9216 (2006).
5. C. Karnutsch, M. Stroisch, M. Punke, U. Lemmer, J. Wang, and T. Weimann, "„Laser diode-pumped organic semiconductor lasers utilizing two-dimensional photonic crystal resonators," *IEEE Photon. Technol. Lett.* **19**(10), 741–743 (2007).
6. H. Sakata, K. Yamashita, H. Takeuchi, and M. Tomiki, "Diode-pumped distributed-feedback dye laser with an organic–inorganic microcavity," *Appl. Phys. B* **92**(2), 243–246 (2008).
7. Y. Yang, G. A. Turnbull, and I. D. W. Samuel, "Hybrid optoelectronics: A polymer laser pumped by a nitride light-emitting diode," *Appl. Phys. Lett.* **92**(16), 163306 (2008).
8. F. Hide, M. Diaz-Garcia, B. Schwartz, M. Andersson, and A. Heeger, "Semiconducting polymers: a new class of solid-state laser materials," *Science* **273**(5283), 1833–1836 (1996).
9. M. D. McGehee, M. A. Diaz-Garcia, F. Hide, R. Gupta, E. K. Miller, D. Moses, and A. J. Heeger, "Semiconducting polymer distributed feedback lasers," *Appl. Phys. Lett.* **72**(13), 1536 (1998).
10. V. Kozlov, V. Bulovic, P. Burrows, and S. Forrest, "Laser action in organic semiconductor waveguide and double-heterostructure devices," *Nature* **389**(6649), 362–364 (1997).
11. D. Schneider, T. Rabe, T. Riedl, T. Dobbertin, M. Kröger, E. Becker, H.-H. Johannes, W. Kowalsky, T. Weimann, J. Wang, and P. Hinze, "Laser threshold reduction in an all-spiro guest-host system," *Appl. Phys. Lett.* **85**(10), 1659–1661 (2004).
12. N. Tsutsumi, A. Fujihara, and D. Hayashi, "Tunable distributed feedback lasing with a threshold in the nanojoule range in an organic guest-host polymeric waveguide," *Appl. Opt.* **45**(22), 5748–5751 (2006).

13. K. Suzuki, K. Takahashi, Y. Seida, K. Shimizu, M. Kumagai, and Y. Taniguchi, "A continuously tunable organic solid-state laser based on a flexible distributed-feedback resonator," *Jpn. J. Appl. Phys.* **42**(Part 2, No. 3A), L249–L251 (2003).
14. M. R. Weinberger, G. Langer, A. Pogantsch, A. Haase, E. Zojer, and W. Kern, "Continuously color-tunable rubber laser," *Adv. Mater. (Deerfield Beach Fla.)* **16**(2), 130–133 (2004).
15. B. Wenger, N. Tétreault, M. E. Welland, and R. H. Friend, "Mechanically tunable conjugated polymer distributed feedback lasers," *Appl. Phys. Lett.* **97**(19), 193303 (2010).
16. P. Görrn, M. Lehnhardt, W. Kowalsky, T. Riedl, and S. Wagner, "Elastically tunable self-organized organic lasers," *Adv. Mater. (Deerfield Beach Fla.)* **23**(7), 869–872 (2011).
17. S. Döring, M. Kollosche, T. Rabe, J. Stumpe, and G. Kofod, "Electrically tunable polymer DFB laser," *Adv. Mater. (Deerfield Beach Fla.)* **23**(37), 4265–4269 (2011).
18. S. Klinkhammer, T. Woggon, U. Geyer, C. Vannahme, T. Mappes, S. Dehm, and U. Lemmer, "A continuously tunable low-threshold organic semiconductor distributed feedback laser fabricated by rotating shadow mask evaporation," *Appl. Phys. B* **97**(4), 787–791 (2009).
19. M. Stroisch, T. Woggon, C. Teiwes-Morin, S. Klinkhammer, K. Forberich, A. Gombert, M. Gerken, and U. Lemmer, "Intermediate high index layer for laser mode tuning in organic semiconductor lasers," *Opt. Express* **18**(6), 5890–5895 (2010).
20. J. Wang, T. Weimann, P. Hinze, G. Ade, D. Schneider, T. Rabe, T. Riedl, and W. Kowalsky, "A continuously tunable organic DFB laser," *Microelectron. Eng.* **78-79**, 364–368 (2005).
21. F. B. Arango, M. B. Christiansen, M. Gersborg-Hansen, and A. Kristensen, "Optofluidic tuning of photonic crystal band edge lasers," *Appl. Phys. Lett.* **91**(22), 223503 (2007).
22. T. Voss, D. Scheel, and W. Schade, "A microchip-laser-pumped DFB-polymer-dye laser," *Appl. Phys. B* **73**(2), 105–109 (2001).
23. R. Ozaki, T. Shinpo, K. Yoshino, M. Ozaki, and H. Moritake, "Tunable liquid crystal laser using distributed feedback cavity fabricated by nanoimprint lithography," *Appl. Phys. Express* **1**(1), 012003 (2008).
24. S. Klinkhammer, N. Heussner, K. Huska, T. Bocksrocker, F. Geislhöringer, C. Vannahme, T. Mappes, and U. Lemmer, "Voltage-controlled tuning of an organic semiconductor distributed feedback laser using liquid crystals," *Appl. Phys. Lett.* **99**(2), 023307 (2011).
25. T. Woggon, S. Klinkhammer, and U. Lemmer, "Compact spectroscopy system based on tunable organic semiconductor lasers," *Appl. Phys. B* **99**(1-2), 47–51 (2010).
26. S. Klinkhammer, T. Woggon, C. Vannahme, T. Mappes, and U. Lemmer, "Optical spectroscopy with organic semiconductor lasers," *Proc. SPIE* **7722**, 77221I, 77221I-10 (2010).
27. B. Park and M. Y. Han, "Organic light-emitting devices fabricated using a premetered coating process," *Opt. Express* **17**(24), 21362–21369 (2009).
28. C. Ge, M. Lu, X. Jian, Y. Tan, and B. T. Cunningham, "Large-area organic distributed feedback laser fabricated by nanoreplica molding and horizontal dipping," *Opt. Express* **18**(12), 12980–12991 (2010).
29. L. D. Landau and V. G. Levich, "Dragging of a liquid by a moving plate," *Acta Phys. URSS* **17**, 42–54 (1942).
30. M. Lehnhardt, T. Riedl, T. Weimann, and W. Kowalsky, "Impact of triplet absorption and triplet-singlet annihilation on the dynamics of optically pumped organic solid-state lasers," *Phys. Rev. B* **81**(16), 165206 (2010).
31. T. Aimonio, Y. Kawamura, K. Goushi, H. Yamamoto, H. Sasabe, and C. Adachi, "100% fluorescence efficiency of 4,4'-bis[(N-carbazole)styryl]biphenyl in a solid film and the very low amplified spontaneous emission threshold," *Appl. Phys. Lett.* **86**(7), 071110 (2005).
32. A. Boudrioua, P. A. Hobson, B. Matterson, I. D. W. Samuel, and W. L. Barnes, "Birefringence and dispersion of the light emitting polymer MEH-PPV," *Synth. Met.* **111-112**, 545–547 (2000).
33. M. Campoy-Quiles, G. Heliotis, R. Xia, M. Ariu, M. Pintani, P. Etchegoin, and D. D. C. Bradley, "Ellipsometric characterization of the optical constants of polyfluorene gain media," *Adv. Funct. Mater.* **15**(6), 925–933 (2005).

1. Introduction

Organic semiconductor lasers have attracted a lot of interest since the first realization of lasing in 1996 [1,2]. The broad spectral gain of active organic semiconductor materials enables the realization of laser devices with emission within the whole visible spectrum by using only a few active materials. Further advantages are efficient energy conversion which allows optical pumping with laser diodes [3–6] or light emitting diodes [7] and the simplicity of fabrication. Especially lasers relying on distributed feedback (DFB) exhibit low thresholds and single longitudinal mode emission. Thin films of the active material are either obtained by processing solutions of conjugated polymers [8,9] or evaporating small molecules [10,11] on top of the substrates with surface gratings. Continuous tunability of such solid-state organic DFB lasers has already been demonstrated with several approaches such as holographic dynamic DFB gratings [12], stretchable DFB lasers [13–17], a wedge-shaped film of either the gain material layer [18] or an intermediate high-index layer [19], a continuously changing grating period [20], optofluidic tuning [21], tuning the temperature of the device [22] or DFB lasers that incorporate liquid crystals [23,24]. Furthermore, the general applicability of a wedge-

shaped organic DFB laser using evaporated small molecules with a continuous tuning range of up to 25 nm has been demonstrated in spectroscopic and laser-induced fluorescence measurements [25,26]. Organic semiconductor DFB laser chips with a spatially varying lasing wavelength can be tuned quickly by using a pump pulse synchronized rotation scheme [25]. In both cases, the thickness gradient of the active layer was fabricated by thermally co-evaporating the small molecule tris(8-hydroxyquinoline) aluminum (Alq₃) and the laser dye 4-dicyanmethylene-2-methyl-6-(p-dimethylaminostyryl)-4H-pyran (DCM) with a rotating shadow mask evaporation technique. This approach, however, is limited to small molecules and cannot be utilized for solution processable materials. Hence, we investigated a new technique for the solution-based fabrication of thin films with a thickness gradient.

In this manuscript, we demonstrate the fabrication of continuously tunable DFB lasers from solution. This is achieved by using a pre-metered coating process (“horizontal-dipping”) to deposit thin films of various conjugated polymer solutions and blended solutions with a thickness gradient on large-scale surface grating samples [27,28]. We deposited three different active material solutions and obtained continuous tunability in the blue, green and red spectral region on a single chip each. The achieved low lasing-thresholds allow pumping using a low-cost, compact laser diode which enables hybrid inorganic-organic continuously tunable laser sources.

2. Device design and fabrication processes

The lasing wavelength of a DFB laser can be approximated by $\lambda_{las} \approx 2 \Lambda n_{eff} / m$. The order of diffraction which provides the resonant feedback is described by m , n_{eff} is the refractive index of the resonant mode and Λ is the corrugation period. In the case of second order DFB lasers, optical feedback is provided by second-order Bragg diffraction while laser emission is coupled out perpendicularly off the sample by first-order Bragg diffraction. The effective refractive index n_{eff} of the propagating slab waveguide mode depends on the active layer thickness, the refractive indices of the different layers and the geometrical details of the grating. Hence, an increase of the film thickness results in an increase of the lasing wavelength.

We used grating samples with different surface corrugation periods. For the red emitter, a period of $\Lambda = 390$ nm was chosen, for the green emitter $\Lambda = 350$ nm and for the blue emitting material the grating constant was $\Lambda = 270$ nm. The former two grating samples were fabricated with a combination of laser interference lithography and reactive ion etching (RIE) [18]. As substrate material, we used quartz glass plates (GE124) with dimensions of 25 mm x 25 mm. While the 390 nm-grating was a simple line grating, we fabricated a two-dimensional photonic crystal lattice in the case of the period of 350 nm by subsequently exposing the sample to the interfering laser beams at 0° and 90°. The sample with the period of 270 nm was fabricated with a combination of electron beam exposure and subsequent RIE. The grating was 3 mm x 10 mm in size.

The horizontal dipping apparatus consists of a cylindrical rod as coating barrier which is mounted parallel with its long axis in a small, defined distance h with respect to the grating sample surface. The gap h between the barrier and the substrate is filled with the organic solution with a syringe upon which a meniscus forms. The sample is mounted horizontally on a vacuum chuck on a two-axis tilt-stage. A motorized translation stage (Emis GmbH, SM42051) controlled by a motion controller (Trinamic GmbH, TCMC-310) moves the coating barrier and thus also the meniscus parallel to the grating surface at a defined speed v . According to Ref [29], the film thickness d in such a deposition process can be estimated using

$$d = 1.34 \cdot \left(\frac{\mu v}{\sigma} \right)^{2/3} \cdot R_d \quad (1)$$

with the viscosity μ , the surface tension σ and the radius of curvature of the meniscus R_d . The translation speed v defines the resulting film thickness. This method is capable of producing large-area homogeneous films from solution [28].

As active material solutions we used the conjugated polymers poly[(9,9-dioctylfluorenyl-2,7-diyl)-alt-co-(1,4-benzo-[2,1',3]-thiadiazole)] (F8_{0,9}BT_{0,1},

ADS133YE, American Dye Source, Inc.) and poly[(9,9-dioctylfluorenyl-2,7-diyl)-co-(1,4-benzo-{2,1',3}-thia-diazole)] (F8BT, ADS233YE, American Dye Source, Inc.) dissolved in toluene at concentrations of 30 mg/ml for the green emission and a blend of F8_{0.9}BT_{0.1} or F8BT and the conjugated polymer poly[2-methoxy-5-(2-ethylhexyl-oxy)-1,4-phenylene-vinylene (MEH-PPV, American Dye Source, Inc.) dissolved in toluene at a concentration of 20 mg/ml (85:15 wt%) for the red emission [30]. As laser material emitting in the blue spectral region, we dissolved poly(9-vinylcarbazole) (PVK, Sigma Aldrich), 4,4'-di(N-carbazolyl)biphenyl (CBP, Sigma Aldrich) and 4,4'-bis[(N-carbazole)styryl]biphenyl (BSB-Cz, own synthesis) in toluene at a concentration of 32 mg/ml (55:37.5:7.5 wt%). BSB-Cz is known to be an efficient, high-gain small-molecule laser material in the blue spectral region [31]. After dissolving, we filtered this solution by using a 0.45 μm microporous membrane filter as this improved the film quality.

For the fabrication of thin films with continuously changing thickness using the horizontal dipping process, the translation of the coating barrier along the sample is accelerated which gives a position dependent barrier velocity and thus, a position dependent film thickness on the sample. The resulting structure is schematically shown in Fig. 1(a). The photograph in Fig. 1(b) shows a sample without surface grating that was coated with the F8_{0.9}BT_{0.1}:MEH-PPV-blend. A spatially varying color which evolves from wedge-shaped thin film interference effects is visible.

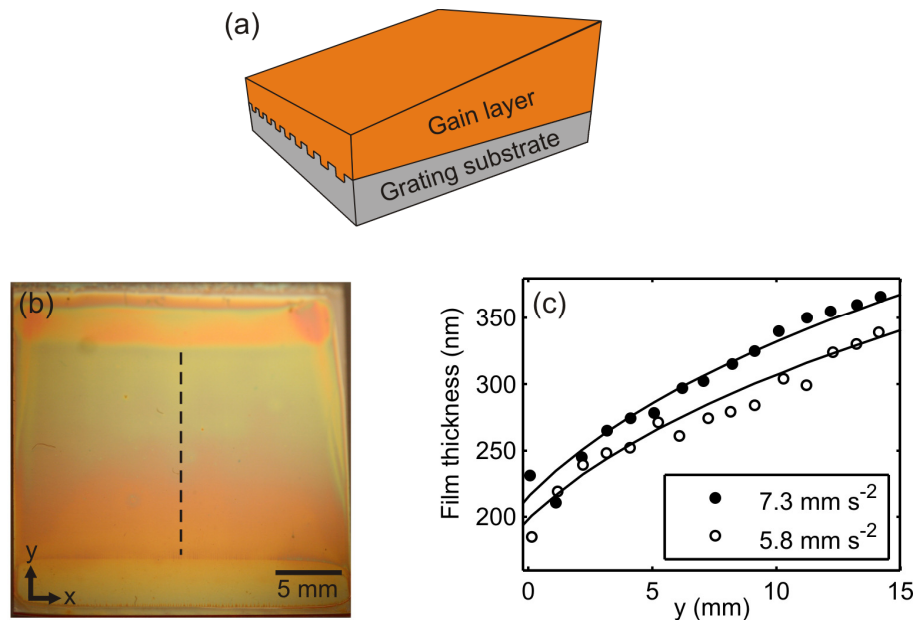


Fig. 1. (a) Scheme of the wedge-shaped organic DFB laser. (b) Photograph of a glass plate with a continuously changing film thickness of a conjugated polymer blend coated by horizontal dipping. (c) Film thickness profile for two samples coated using with different barrier accelerations of 5.8 mm s⁻² and 7.3 mm s⁻² as measured (symbols) and numerically fitted (solid lines).

The photograph also shows that both start (bottom) and end (top) region of the coating process are inhomogeneous. In the start region the film thickness is uncontrolled as this is the part of the sample where the meniscus is initially formed before the coating barrier is moved. The thickness at the end region cannot be controlled either as the meniscus is interrupted when passing the edge of the sample which leads to an uncontrolled back flow of the solution. Thus, we disregarded these both regions in our measurements. In Fig. 1(c), we plotted two film thickness profiles along the thickness gradient in the central, unperturbed region. For this, the thin film was scratched along the dotted line and measured with a surface profiler (Veeco Instruments Ltd., Dektak V 220-Si). We obtained the thickness gradient by using coating accelerations of 5.8 mm s⁻² and 7.3 mm s⁻² on plane soda-lime glass substrates which gave thicknesses from about 200 nm to 350 nm and 390 nm respectively. In all cases, we used a gap height of $h = 0.8$ mm for our

experiments. The obtained profiles are in good agreement with the theoretical model from Eq. (1) with $(\mu/\sigma)^{2/3} \cdot R_d$ as common fitting parameter.

3. Optical characterization

For optical characterization of the fabricated DFB lasers the samples were optically excited by a diode-pumped, actively Q-switched frequency tripled neodymium:yttrium-orthovanadate (Nd:YVO₄) laser (Advanced Optical Technology Ltd., AOT-YVO-20QSP) with a wavelength of 355 nm. The pump pulses had a duration of approximately 0.5 ns at a repetition rate of 1.4 kHz. The pump pulse energy was adjusted with a variable neutral density filter and measured with a calibrated gallium arsenide phosphide photodiode connected to an oscilloscope (Tektronix, TDS2024). The sample was kept in a vacuum chamber ($<5 \times 10^{-5}$ mbar) to protect the active material from photooxidation. Emission from the sample was collected using the focusing lens, then directed through a dichroic mirror and coupled into a multimode optical fiber and further on to a spectrograph (Acton Research Corporation, SpectraPro 300i, variable grating) connected to an intensified charge-coupled device camera (Princeton Research, PiMax 512). The vacuum chamber containing the samples could be moved in the plane perpendicular to the pump beam using an automated precision stage. This allowed for a spectrally and spatially resolved characterization of the samples.

Figure 2(a) shows the lasing spectra on a sample with a linear grating and a period of $\Lambda = 390$ nm coated with the red-emitting polymer-blend F_{80.9}BT_{0.1}:MEH-PPV using an acceleration of 7.3 mm s^{-2} . We obtained the spectra by moving the sample relative to the pump spot parallel to the thickness gradient. We measured a continuous tunability from 596 nm to 615 nm in those regions of the sample that were not affected by thickness inhomogeneities in the start region and the backflow area. Lasing thresholds were as low as $3.8 \text{ nJ pulse}^{-1}$ at elliptical pump spot dimensions of $160 \mu\text{m} \times 180 \mu\text{m}$, as shown in Fig. 2(b). This gives a minimum threshold energy density of $16.8 \mu\text{J cm}^{-2}$.

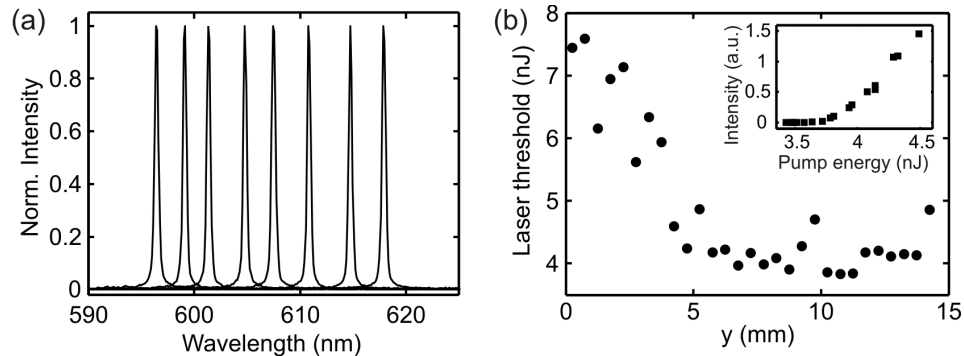


Fig. 2. (a) Laser spectra measured at different pump spot positions along the thickness gradient on the wedge-shaped DFB laser with F_{80.9}BT_{0.1}:MEH-PPV as gain material. (b) Lasing thresholds for different positions and thus, different film thicknesses. Inset: Input-output characteristic of the DFB laser at a wavelength of 612.6 nm.

Figure 3(a) shows a color encoded plot of the spatially resolved lasing wavelengths of the TE₀-mode. In order to obtain this graph, the sample was scanned relatively to the pump spot with a spatial resolution of $250 \mu\text{m}$ and a spectrum was taken at each point.

We fabricated two identical samples and measured the spatially resolved lasing wavelengths on both samples in our optical setup in order to check the reproducibility of the film thickness variation and the corresponding continuous laser wavelength tuning. The average position dependent lasing wavelength along with the standard deviation is shown in Fig. 3(b) for the whole lasing area of the two samples.

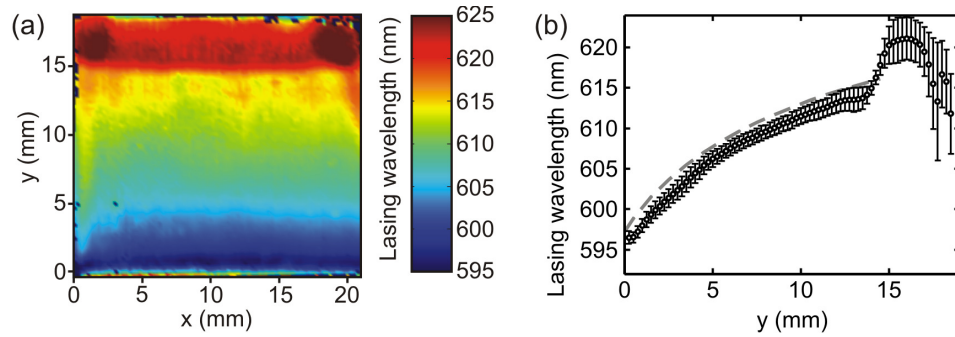


Fig. 3. (a). Spatially resolved lasing wavelength of the TE₀-mode. (b) Position-dependent averaged lasing wavelength and standard deviation along the gradient determined from two identical samples (black). Expected position-dependence of lasing wavelength using the measured thickness profile and the Bragg condition (dashed gray).

We find a mean standard deviation of the lasing wavelength of about 1.0 nm. Furthermore, it is observed that the deviation is strongest close to the backflow regions as already pointed out in section 1. Figure 3(b) also contains the expected lasing wavelengths using the Bragg condition with the thickness profile from Fig. 1(c). The refractive index dispersion of MEH-PPV was taken from Ref. 32. We assumed F8_{0.9}BT_{0.1} to have the same refractive index dispersion as poly(9,9-dioctylfluorene) (PFO) which was taken from Ref. 33.

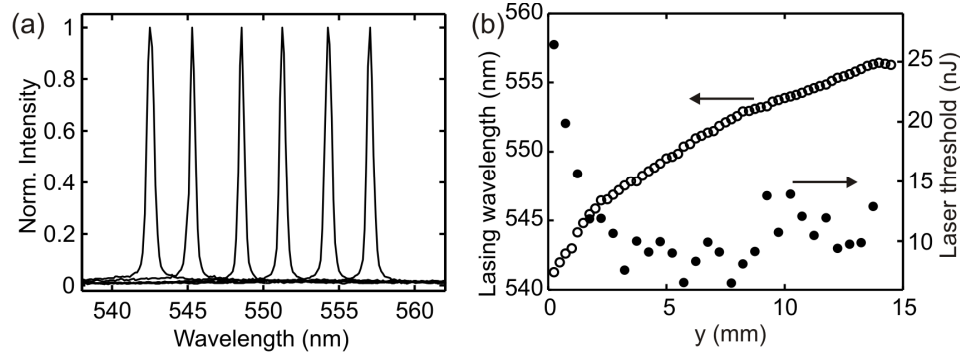


Fig. 4. (a). Laser spectra measured at different pump spot positions along the thickness gradient on the wedge-shaped DFB laser with F8_{0.9}BT_{0.1} as gain material. (b) Position-dependent lasing wavelengths and lasing thresholds along the thickness gradient.

In order to demonstrate the versatility of this method, we also coated the green emitting polymer F8_{0.9}BT_{0.1} dissolved in toluene onto the two-dimensional photonic crystal lattice at an acceleration of 7.3 mm s⁻². The obtained gradient showed lasing from about 541 nm to 557 nm, as shown in Figs. 4(a) and 4(b). The lowest threshold obtained was 6.5 nJ pulse⁻¹ at a wavelength of 552 nm. The size of the elliptical pump spot was 160 μm x 180 μm so that the minimum threshold energy density is 28.7 μJ cm⁻².

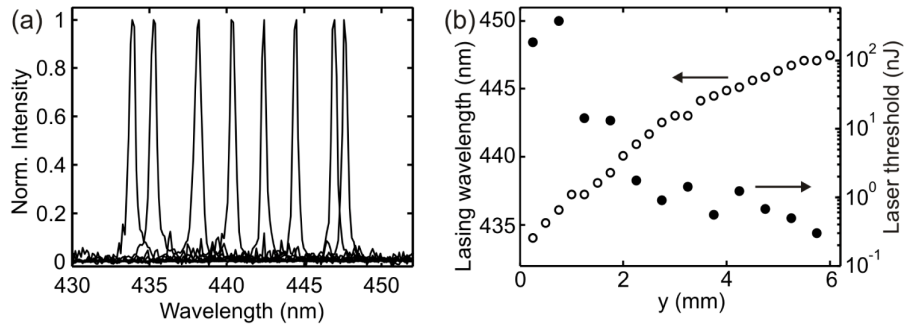


Fig. 5. (a). Laser spectra measured at different pump spot positions along the thickness gradient on the wedge-shaped DFB laser with PVK:CBP:BSB-Cz as gain material. (b) Position-dependent lasing wavelengths and lasing thresholds along the thickness gradient.

Additionally to conjugated polymer materials, horizontal dipping is also feasible for the deposition of solutions containing small molecules. A blue-emission spectrally tunable DFB laser was fabricated by depositing a blend of PVK:CBP:BSB-Cz dissolved in toluene onto a silicon dioxide grating with a grating period of $\Lambda = 270$ nm. The coating barrier was accelerated with 5.8 mm s^{-2} . We obtained tunability from about 434 nm to 447 nm and a minimum threshold of about $0.5 \text{ nJ pulse}^{-1}$ at a pump spot size of $70 \mu\text{m} \times 120 \mu\text{m}$ as shown in Figs. 5(a) and (b) respectively. The minimum threshold energy density is $7.6 \mu\text{J cm}^{-2}$.

4. Laser diode pumping

As optical pump source, we used a commercially available low-cost 1 W laser diode ($\lambda = 445$ nm) and a pulsed power supply (Picolas GmbH, LDP-V-50100) to generate laser pulses with a pulsewidth of 20 ns at a repetition rate of 100 Hz. When using such short pulsewidths, the laser diode can be driven at high peak current levels of up to 20 A resulting in an optical pulse energy of 367 nJ in the sample chamber (see Fig. 6(c)). With this pump source we obtained tunable laser emission from a wedge-shaped, blended F8BT:MEH-PPV polymer film on a grating substrate (Fig. 6(a)). To reduce the laser threshold, we enhanced the absorption of pump light by placing a dichroic mirror on top of the polymer film and pumping through the transparent grating substrate, allowing for a second pass of the non-absorbed pump light through the gain medium. In Fig. 6(b), the position dependent lasing wavelength giving a tuning range of about 11 nm is shown. The input-output-curve of the laser emission at a wavelength of 635 nm is shown in Fig. 6(c). We measured the absolute emitted pulse energy with a pulse energy meter (Coherent, Labmax-TOP, J-10MT-10kHz EnergyMax Pyroelectric Sensor) and found a slope efficiency of 1.2% for this wavelength. Figure 6(d) shows a photograph of the generated DFB laser emission on a paper screen.

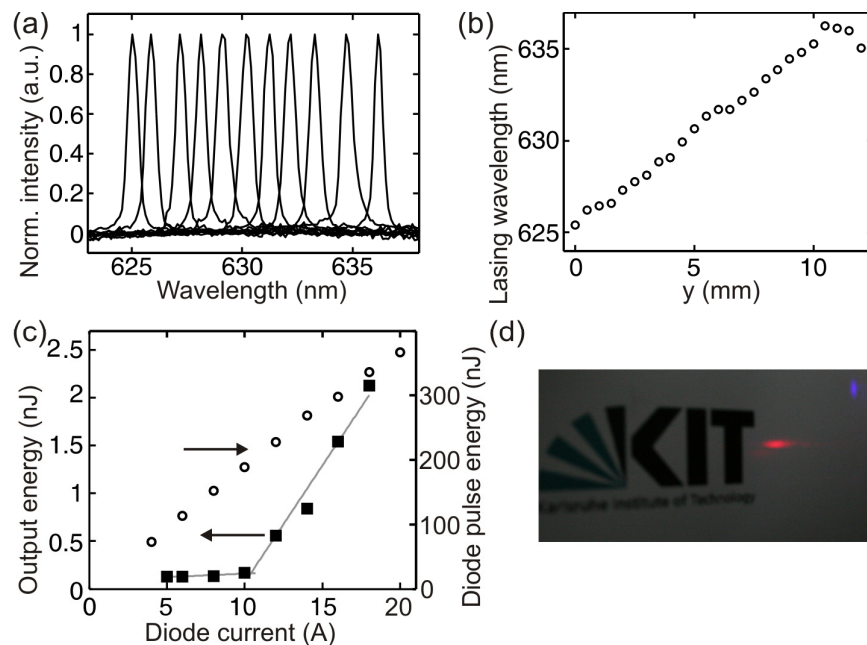


Fig. 6. (a). Laser spectra measured at different pump spot positions along the thickness gradient on the wedge-shaped DFB laser with F8BT:MEH-PPV as gain material and a laser diode as pump source. (b) Position-dependent lasing wavelengths along the thickness gradient. (c) Input-output characteristic of the DFB laser emitting at 634 nm pumped with a laser diode (squares) and current-output energy characteristics of the pulsed laser diode (circles). (d) Photograph of the DFB laser emission on a paper screen.

5. Conclusion

In summary, we fabricated thin organic semiconductor films of continuously varying thickness from solution by accelerating the coating barrier in the horizontal dipping coating process. By this, we realized continuously tunable DFB laser emission from three different samples each coated with a different organic gain material emitting in the blue, green and red spectral region. In the blue spectral region we obtained a tunability of 13 nm, in the green 16 nm and in the red 19 nm. The low thresholds enable pumping of a red emitting device with a compact blue-emitting laser diode. This enables potential applications of wedge-shaped organic DFB lasers for compact, low-cost, continuously tunable hybrid inorganic-organic laser diodes.

Acknowledgments

The authors would like to thank Mario Süttsch for support with the construction of the horizontal dipping apparatus. We thank Jing Becker and Thomas Weimann for providing the SiO₂-grating substrates. This work was supported by the Deutsche Forschungsgemeinschaft and the State of Baden-Württemberg through the subproject A 4.10 of the DFG-Forschungszentrum "Center for Functional Nanostructures" (CFN). The work of S.K., X.L., Y.S., and C.V. is supported by the Karlsruhe School of Optics and Photonics (KSOP). X.L. acknowledges financial support from the Carl Zeiss Stiftung. T.M.'s Young Investigator Group received financial support from the "Concept for the Future" of the Karlsruhe Institute of Technology within the framework of the German Excellence Initiative.